Cell Stem Cell
Short Article

Derivation Conditions Impact X-Inactivation Status in Female Human Induced Pluripotent Stem Cells

Kiichiro Tomoda,[1] Kazutoshi Takahashi,[3] Karen Leung,[2] Aki Okada,[3] Megumi Narita,[3] N. Alice Yamada,[4] Kirsten E. Eilertson,[1] Peter Tsang,[4] Shiro Baba,[1] Mark P. White,[1] Salma Sami,[1] Deepak Srivastava,[1] Bruce R. Conklin,[1] Barbara Panning,[2,*] and Shinya Yamanaka[1,3,*]
[1]Gladstone Institute of Cardiovascular Disease
[2]Department of Biochemistry and Biophysics
University of California, San Francisco, San Francisco, CA 94158, USA
[3]Center for iPS Cell Research and Application (CiRA), Kyoto University, Kyoto 606-8507, Japan
[4]Agilent Laboratories, Agilent Technologies, Santa Clara, CA 95051, USA
*Correspondence: barbara.panning@ucsf.edu (B.P.), syamanaka@gladstone.ucsf.edu (S.Y.)
DOI 10.1016/j.stem.2012.05.019

SUMMARY

Female human induced pluripotent stem cell (hiPSC) lines exhibit variability in X-inactivation status. The majority of hiPSC lines maintain one transcriptionally active X (Xa) and one inactive X (Xi) chromosome from donor cells. However, at low frequency, hiPSC lines with two Xas are produced, suggesting that epigenetic alterations of the Xi occur sporadically during reprogramming. We show here that X-inactivation status in female hiPSC lines depends on derivation conditions. hiPSC lines generated by the Kyoto method (retroviral or episomal reprogramming), which uses leukemia inhibitory factor (LIF)-expressing SNL feeders, frequently had two Xas. Early passage Xa/Xi hiPSC lines generated on non-SNL feeders were converted into Xa/Xa hiPSC lines after several passages on SNL feeders, and supplementation with recombinant LIF caused reactivation of some of X-linked genes. Thus, feeders are a significant factor affecting X-inactivation status. The efficient production of Xa/Xa hiPSC lines provides unprecedented opportunities to understand human X-reactivation and -inactivation.

INTRODUCTION

Female human induced pluripotent stem cell (hiPSC) and human embryonic stem cell (hESC) lines with two active X chromosomes (Xas) occur infrequently, and Xa/Xa hESC lines often become Xa/Xi (Bruck and Benvenisty, 2011; Cheung et al., 2011; Fan and Tran, 2011; Hanna et al., 2010; Hoffman et al., 2005; Lagarkova et al., 2010; Lengner et al., 2010; Marchetto et al., 2010; Pomp et al., 2011; Shen et al., 2008; Silva et al., 2008; Tchieu et al., 2010; Teichroeb et al., 2011). However, some Xa/Xa hESC lines do not exhibit X-inactivation upon differentiation (Hoffman et al., 2005). The reasons for this variability are not fully understood, but it is known that derivation and culture conditions affect epigenetic features of X chromosomes (Hanna et al., 2010; Lengner et al., 2010; Pomp et al., 2011; Ware et al., 2009).

This study investigated the X-inactivation status of hiPSCs derived by the Kyoto method, which uses SNL feeder cells that produce high levels of leukemia inhibitory factor (LIF) (McMahon and Bradley, 1990; Nakagawa et al., 2008; Takahashi et al., 2007). We report here that the Xi of donor fibroblasts was frequently reactivated in hiPSC lines generated on SNLs. Early passage hiPSC lines were Xa/Xi and converted into Xa/Xa lines upon continued passage on SNL feeders, but not on non-SNL feeders. Lines cultured on non-SNL feeders supplemented with recombinant (r)LIF had features of X-reactivation. These data indicate that feeder cells significantly affect X-inactivation status and that LIF contributes to reactivation. Reliably generating hiPSCs with the desired Xa/Xi or Xa/Xa pattern would be useful in disease modeling and clinical applications.

RESULTS

X-Linked Genes Are Highly Expressed in Female hiPSC Lines

We used microarrays to examine X-linked gene expression in hiPSC lines derived from differentiated H9 ESCs (H9-reporter) (Figures 1A and 1B, S1A–S1I available online; and Table S1) or human fibroblasts (hFibs) (Figures 1D and 1E, S1J–S1Q; and Table S1). Approximately 40% of X-linked genes were expressed at >1.5-fold levels in female hiPSC lines than in Xa/Xi or XY hESC lines (Figure 1C). Plotting the expression ratios of female hiPSCs and hESCs onto the human genome revealed that the X was the only chromosome with chromosome-wide upregulation in hiPSCs (Figure 1F). Thus, X-linked genes are specifically upregulated in female hiPSCs derived from differentiated hESCs or hFibs, suggesting X-reactivation in female hiPSCs.

Two Xs Are Active in Female hiPSCs

We next examined expression of two X-linked genes, *PGK1* and *XIST*, by fluorescent in situ hybridization (FISH). We found that >60% of hiPSCs had two sites of nuclear transcript accumulation for *PGK1*, in contrast to an Xa/Xi hESC line, which had only one site in ~60% of cells (Figures 2A and 2B). XIST RNA coating and high expression were detected in Xa/Xi hESCs, but not in

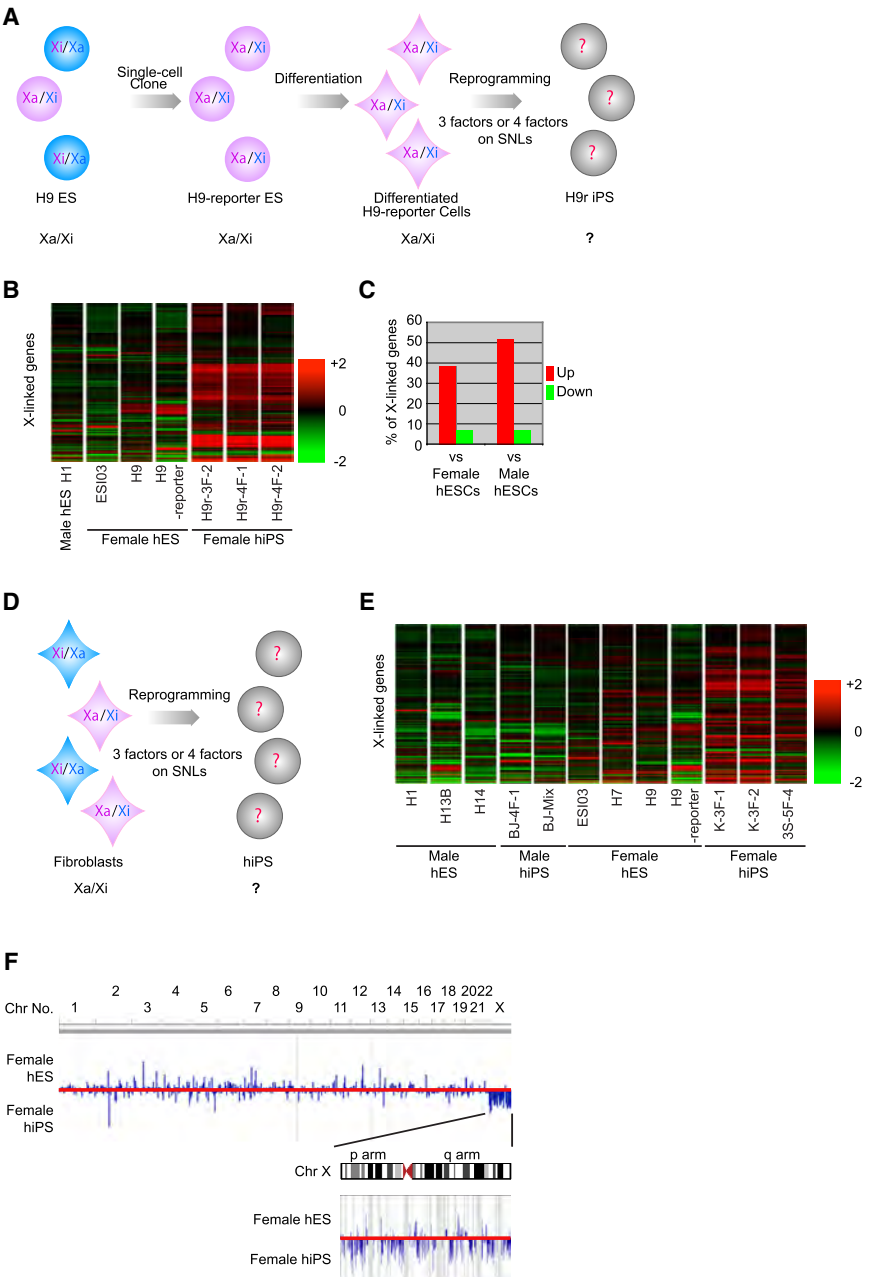

Figure 1. X-Linked Genes Are Highly Expressed in Female hiPSC Lines

(A and D) Experimental design to generate hiPSC lines from H9 ESCs (A) and from hFibs (D). The X-inactivation status of the each cell line is also shown. The characterizations of the hiPSC lines are shown in Figure S1 and Table S1.

(B and E) Heat maps of relative expression levels of the X-linked genes. All cell lines were cultured in identical conditions. RNA was extracted from H9r iPSC lines at p3 and female hiPSC lines from hFibs at >p15.

(C) Percentage of all X-linked genes (probes) that are upregulated (red) or downregulated (green) by more than 1.5-fold in the H9r iPSC lines and female (Xa/Xi) hESC lines (average data among ESI03, H9-reporter, and H9) or the male (XY) ESC H1 cell line.

(F) Gene expression ratios on the genome. The expression ratios between female hESC (average data among ESI03, H7, H9, and H9-reporter) and hiPSC (average data among K-3F-1, K-3F-2, and 3S-5F-4) lines are plotted on human genome. Blue bars indicate where each gene maps. Blue bars above the red midline show highly expressed genes in the hESC lines. Blue bars below the midline show highly expressed genes in the hiPSC lines. The height of bars indicates the expression ratio of each gene. Chromosome numbers are shown on top of the diagram. The Y chromosome is excluded in this assay. The X chromosome is expanded in the inset.

In (B) and (E), gene expression values for each gene are shown in $\log_2$ scale.

hiPSCs (Figures 2A and 2C). In addition, a majority of hiPSCs exhibited RNA polymerase II (polII) staining on both Xs, while hESCs exhibited staining on one X (Figure 2D), indicating that these hiPSC lines have two Xas.

The X-linked gene *WDR44* showed greater levels of expression in hiPSCs (H9r iPSCs), which were derived from differentiated H9-reporter cells, than in H9-reporter ESCs (Figure 2E, left) and was biallelically expressed only in H9r iPSCs as detected by single nucleotide polymorphism (SNP) sequencing (Figure 2E, right). Bisulfite sequencing of the *WDR44* promoter showed that hESCs had a mixed methylation pattern characteristic of Xa/Xi cell lines (Heard and Disteche, 2006; Shen et al., 2008), while hiPSCs were hypomethylated (Figure 2F).

Finally, we used X to autosome expression ratios (X/A ratios): Xa/Xi cell lines have lower X/A ratios than Xa/Xa cell lines (Bruck and Benvenisty, 2011; Lin et al., 2007; Nguyen and Disteche, 2006). X/A ratios derived from deposited microarray data sets from hiPSC and hESC lines in which X-inactivation status is already characterized (Hanna et al., 2010; Lengner et al., 2010; Tchieu et al., 2010) were well correlated with X-inactivation status (Figure 2G, left three lanes). We found that X/A ratios from our female hiPSCs were comparable to those of reported Xa/Xa cells. These results confirmed X-reactivation in hiPSCs and indicate that X/A ratios provide a useful method of identifying potential Xa/Xa hiPSC lines.

One X Is Inactivated upon Differentiation of Female hiPSCs

We analyzed a pure population of cells differentiated into endothelial cells. Xa/Xa hiPSC-derived endothelial cells exhibited low X/A ratios, comparable to primary endothelial cells and those differentiated from male or Xa/Xi hESCs (Figure 2H). XIST RNA was not detected, while only a single site of nascent *PGK1* transcript accumulation was detected in >60% of Xa/Xa-derived endothelial cells (Figures 2I and 2J). These results indicate that one X is silenced after differentiation of Xa/Xa hiPSCs.

Prolonged Culture Promotes X-Reactivation in hiPSCs Derived and Propagated on SNL Feeders

We analyzed X-inactivation status in more hFib-derived hiPSC lines generated on SNLs by three- or four-factor viral reprogramming or integration-free episomal vector reprogramming (Okita et al., 2011) (Table S1). At early passage (passage 5, or p5), X/A ratios of all lines analyzed were consistent with those of reported Xa/Xi lines (Figure 3A, at p5 on SNLs). At late passage (>p15), 20 of 23 lines exhibited high X/A ratios (X/A > 0.3), comparable to those reported for Xa/Xa cells (Figure 3A, at >p15 on SNLs). Two cell lines at >p15 were further analyzed for X-inactivation by FISH, and the majority of cells showed two sites of nuclear transcript accumulation for *PGK1* and no XIST RNA accumulation, indicating that these lines are also Xa/Xa (Figure 3B). Further, Xa/Xa status was maintained with continued passage (Table S1). These results suggest that our method frequently produces stable Xa/Xa hiPSCs.

By microarray analysis, *XIST* expression in all female hiPSCs on SNLs at early passage was similar to that of the donor Xa/Xi hFibs. At late passage, *XIST* was downregulated. We confirmed these findings by quantitative RT-PCR (Figure 3C). Also, SNP sequencing revealed that two X-linked genes (*TSPAN6* and *FRMPD4*) are monoallelically expressed at early passage but biallelically expressed at late passage of hiPSCs on SNLs (Figure 3D). These SNP sequencing results, together with the X/A ratios and *XIST* expression, indicate that the Xi is silent at early passage but is reactivated with continued propagation, concomitant with downregulation of *XIST*.

Feeder Cells Affect X-Inactivation Status in Female hiPSCs

Most female hiPSC lines reprogrammed with our protocol were Xa/Xa, but other laboratories reported Xa/Xi hiPSC lines derived using the same reprogramming factors (Hanna et al., 2010; Pomp et al., 2011; Tchieu et al., 2010). A notable difference between protocols is the type of feeder cells employed. We used SNLs, which are immortalized mouse embryonic fibroblasts that express a LIF transgene (Takahashi et al., 2007), while other laboratories predominantly use mouse primary embryonic fibroblasts (MEFs) (Hanna et al., 2010; Pomp et al., 2011; Tchieu et al., 2010). Thus, we analyzed female hiPSC lines generated on non-SNLs, hFibs (Takahashi et al., 2009), or MEFs (Tchieu et al., 2010) (Table S1). None of the hiPSC lines derived on non-SNLs (0/12) had high X/A ratios (>0.3) at >p15 (Figure 3A, at >p15 on non-SNLs). Three lines were analyzed by FISH, and the majority of cells had only one site of PGK1 nascent mRNA accumulation with or without XIST RNA coating (Figures 3E and 3F). Therefore, hiPSCs generated on non-SNLs retain one Xi as reported (Pomp et al., 2011; Tchieu et al., 2010).

SNLs Have a Role in X-Reactivation in Female hiPSCs

Since LIF is secreted by SNLs, we examined its role on X chromosome-wide gene expression by our protocol. Female hiPSC lines were initially generated on non-SNLs (hFibs or MEFs) and transferred to SNLs or non-SNLs plus rLIF (Figure 4A). For hiPSCs generated on hFibs, transfer occurred at p9. For hiPSCs generated on MEFs, transfer occurred at p1, when hiPSC colonies were initially picked. Female hiPSC lines transferred to SNLs had increased X/A ratios, concomitant with downregulated *XIST* and upregulated X-linked genes. None of the sister lines continually cultured on non-SNLs had substantially increased X/A ratios, suggesting they remained Xa/Xi (Figures 4B–4D, S3A, and S3B). The two hiPSC lines generated on MEFs and transferred to SNLs had X/A ratios similar to those generated and cultured on SNLs and biallelic expression of *TSPAN6* and *FRMPD4* (Figures 4C and 4E). While the hiPSC lines generated on hFibs and transferred to SNLs had increased X/A ratios, the ratios were lower than when hiPSCs were derived exclusively on SNLs, which may be a consequence of initial reprogramming on hFibs and/or the later transfer to SNLs (Figure 4B). In support of the timing of transfer affecting X-inactivation status, one of four hiPSC lines generated on MEFs and transferred to SNLs at p4 or p7 had features of X-reactivation (Figures S3D and S3E). Thus, culture on SNLs can convert early passage Xa/Xi hiPSCs generated and cultured on non-SNLs into Xa/Xa hiPSCs.

Two of four hiPSC lines generated on non-SNLs and transferred to non-SNLs plus rLIF had increased X/A ratios, concomitant with downregulation of *XIST* and upregulation of X-linked genes (Figures 4B, 4C, 4F and S3A and S3B). In a line derived on hFibs and transferred to hFibs plus rLIF at p9, the X/A ratio was comparable to that of the sister line after transfer to SNLs (Figure 4B). The line derived on MEFs and transferred to MEFs plus rLIF at p1 had a lower X/A ratio than its sister line that was transferred to SNLs at p1. While transfer to SNLs elicited biallelic expression of *FRMPD4* and *TSPAN6* (Figure 4E), transfer to MEFs plus rLIF caused biallelic expression of *PGK1* (Figure 4G) and *FRMPD4*, but not *TSPAN6* (Figure 4H), suggesting that rLIF promotes reactivation of a subset of X-linked genes.

Next we asked if the intermediate X/A ratio in hiPSCs cultured on non-SNLs plus rLIF reflected intermediate X-linked gene expression across the entire chromosome. We plotted expression levels of genes across the X from hiPSCs transferred to either non-SNLs plus rLIF or SNLs normalized to the expression of hiPSCs maintained on non-SNLs for the same number of passages (Figure 4I for MEF hiPSCs and S3C for hFib hiPSCs). There was variability across the X (Figure 4I). Some regions were more similar between the MEF plus rLIF hiPSCs and MEF hiPSCs and other regions were more similar between the MEF plus rLIF hiPSCs and SNL hiPSCs, suggesting that rLIF promotes full reactivation of a subset of X-linked genes. On the remainder of the X, the MEF plus rLIF hiPSCs had expression intermediate to MEF hiPSCs and SNL hiPSCs, which may reflect upregulation of the Xa or X-reactivation upon addition of rLIF. *FRMPD4* lies in a region of intermediate expression, suggesting that, while there is biallelic expression, the reactivated genes may not be expressed as highly in MEF plus rLIF hiPSCs as they are in SNL hiPSCs. Our results indicate that reprogramming with SNL feeders promotes robust X-reactivation, and that LIF may contribute to this epigenetic alteration of the Xi.

DISCUSSION

In this study, we showed that female hiPSCs derived by the Kyoto method, using retroviral or episomal vectors, frequently have two Xas. In female hiPSCs derived from hFibs, the Xi remained silent at early passage, but reactivated later, concomitant with downregulation of *XIST*. Since episomal reprogramming

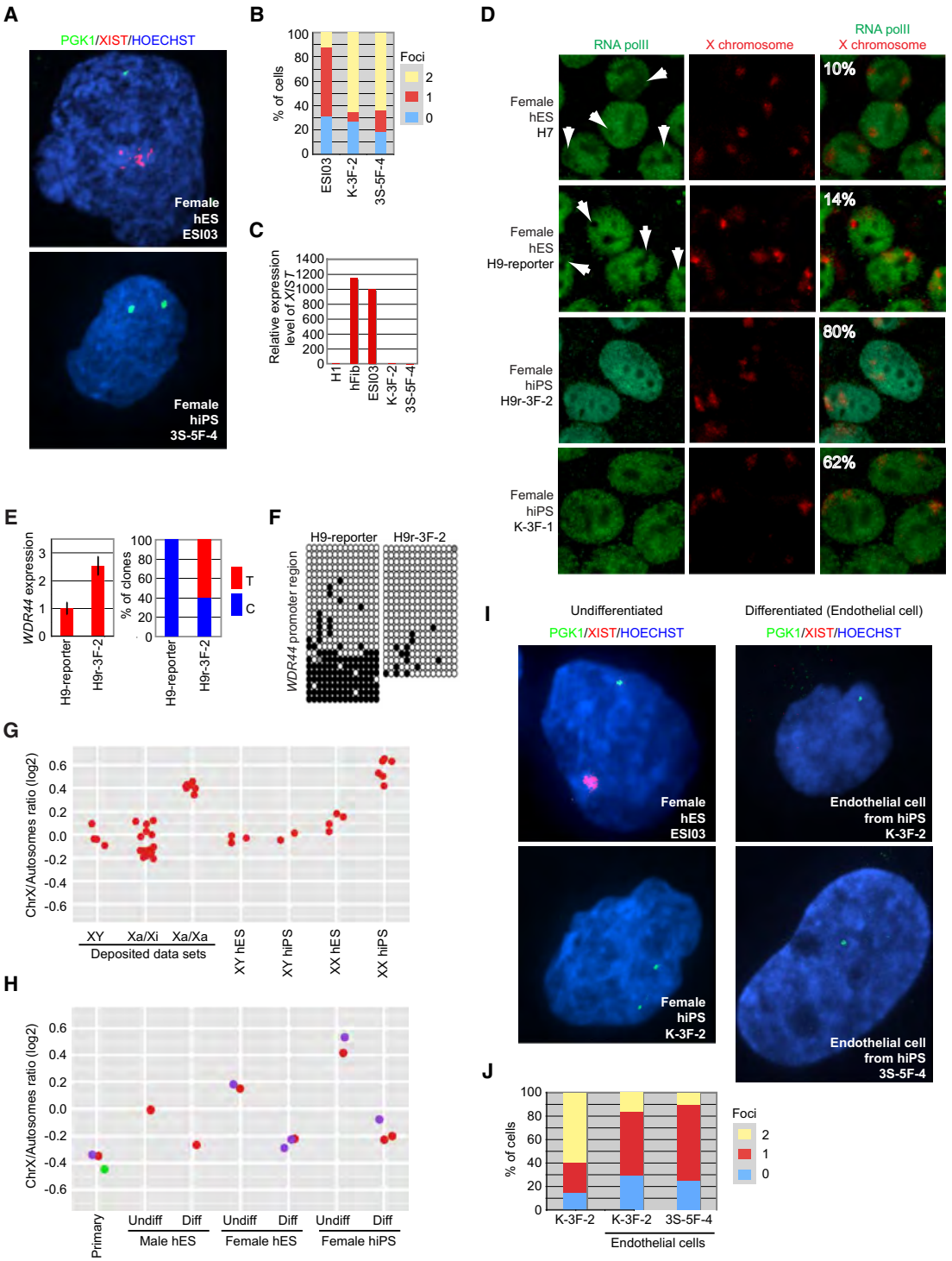

Figure 2. Two Xs Are Active in Female hiPSCs

(A) RNA FISH for *PGK1* (green) and *XIST* (red) in hESCs and hiPSCs derived on SNLs.

(B) Graph showing the proportion of cells with 0, 1, or 2 sites of PGK1 nascent mRNA accumulation in Xa/Xi hESC (ESI03) and female hiPSC (K-3F-2 and 3S-5F-4) lines.

(C) Relative expression levels of *XIST*. The expression levels of *XIST* were extracted from microarray data sets. The male ESC line H1 is used for normalization. Female fibroblasts (hFib) from which the hiPSC lines were generated and Xa/Xi hESCs (ESI03) served as controls.

(D) Immuno-FISH. Representative images for localization of RNA polymerase II (RNA polII) (green) and X chromosomes (red) in the indicated cell lines. Arrows show regions depleted of staining for RNA polII in which one of two X chromosomes localizes. The percentage of cells in which no RNA polII exclusion from an X was observed is inset.

(Okita et al., 2011) supported X-reactivation, neither viral integration nor continued expression of exogenous factors is necessary for this process. Xa/Xa hiPSCs were poised for X-inactivation upon differentiation. The high-frequency X-reactivation and stable Xa/Xa status in hiPSCs derived with the Kyoto method (17/20 retroviral, 3/3 episomal) contrasts with the sporadic or lack of X-reactivation of other methods (Cheung et al., 2011; Hanna et al., 2010; Kim et al., 2011; Lagarkova et al., 2010; Marchetto et al., 2010; Mekhoubad et al., 2012; Pomp et al., 2011; Tchieu et al., 2010). Thus, this method provides an unprecedented tool to understand epigenetic regulation of X chromosomes in human cells.

SNL Feeders Are Important for X-Reactivation

The Kyoto method uses SNL feeders to derive and maintain hiPSCs. When MEFs or hFibs feeders were used, we did not observe frequent production of Xa/Xa hiPSC lines. However, early passage Xa/Xi hiPSCs generated and cultured on non-SNLs could be converted into Xa/Xa after several passages on SNLs, implicating SNLs in X-reactivation.

SNLs supported production of hiPSCs with two Xas, suggesting a role for LIF in X-reactivation. Indeed, transfer into rLIF-containing medium caused upregulation of X-linked genes and increased X/A ratios in two of four hiPSC lines initially generated on non-SNLs. While transfer to rLIF promoted upregulation of X-linked genes, not all genes were upregulated to the same extent as on SNLs, and some were not upregulated at all. Also, not all genes assayed exhibited biallelic gene expression in hiPSCs cultured with rLIF. Thus, culture with rLIF does not have the same chromosome-wide effects that are seen with culture on SNLs. Thus, SNLs may have activities in addition to LIF that enable frequent and chromosome-wide X-reactivation. One possible activity is glycosylation of LIF: glycosylated LIF may have different roles from nonglycosylated LIF (Blanchard et al., 1998), and rLIF is not glycosylated. Identification of such activities, including LIF glycosylation, is an important future task.

Overexpression of OCT3/4, KLF2, and KLF4 in conjunction with MAPKK and GSK3b inhibitors and rLIF stochastically converts Xa/Xi hiPSCs into Xa/Xa hiPSCs (Hanna et al., 2010). In this study, we showed that expression of exogenous OCT3/4 and KLF4 during culture is not required for reactivation. While our results suggest that LIF contributes to SNL-mediated X-reactivation, the effect of SNLs on MAPK and GSK3b pathways should also be investigated.

The timing of transfer to SNLs may affect X-inactivation status, as transfer of initial hiPSC colonies directly onto SNLs resulted in X-reactivation. In contrast, transfer of four Xa/Xi hiPSCs to SNLs at p15 or later did not promote X-reactivation (data not shown). Since the reprogramming process continues during expansion of iPSC clones (Polo et al., 2010), perhaps early exposure to SNLs during this dynamic stage of reprogramming impacts X-linked gene expression at later passage. Epigenetic alterations acquired during culture without SNLs may render the Xi less responsive to the signals that trigger reactivation.

Implication for Medical Applications

A small number of hiPSC lines fail to reactivate the Xi even on SNL feeders. While these Xa/Xi lines are indistinguishable from Xa/Xa lines in differentiation ability and global expression patterns of autosomal genes, these Xa/Xi lines might not be fully reprogrammed. In mouse, there is a relationship between X-reactivation and the "naive" pluripotent state, in which pluripotent cells efficiently contribute to chimeric embryos (Fan and Tran, 2011; Nichols and Smith, 2009; Payer et al., 2011). If the developmental potential of Xa/Xa hiPSCs is also greater, the insights obtained from the Kyoto method may be advantageous for reliable production of quality hiPSCs for future medical applications. However, when treating X-linked human monogenic diseases, such as Rett syndrome, Xa/Xi hiPSCs in which the Xi carries the mutation would be a more attractive source of material for cell-replacement therapies (Tchieu et al., 2010).

A Model System for Study of X-Inactivation and X-Reactivation in Humans

The efficient X-reactivation in our hiPSC lines is a useful tool for elucidating mechanisms of X-reactivation in human cells. Furthermore, a reliable source of Xa/Xa hiPSC lines poised for X-inactivation provides tools to study this process. X-reactivation and X-inactivation have mainly been examined in mouse systems. However, the mechanisms in human may differ from those in mouse (Maherali et al., 2007; Okamoto et al., 2011; Tchieu et al., 2010; van den Berg et al., 2009). The difficulty in obtaining human embryos and the unstable X-inactivation status in hESCs make it extremely difficult to study X-inactivation in

(E) *WDR44* expression in the indicated cell lines was determined by RT-qPCR (left graph). The expression values in the H9-reporter and expression levels of *GAPDH* were used for normalization. Error bars are standard deviations (n = 2). The right bar graph shows the percentage of clones that contain T or C at the same position in WDR44 mRNA in the indicated cell lines. Five H9-reporter and six H9r-3F-2 clones were sequenced.
(F) Methylation patterns of the *WDR44* promoter in the indicated cell lines. Each circle denotes a CpG sequence in the promoter region. Black circles, methylated CpGs; white circles, unmethylated CpGs; gray circles, mutated CpGs. Each row for each cell line shows each sequenced clone for the cell lines.
(G) Each dot shows the expression ratio between X-linked genes and autosomal genes from each cell line. In the left three lanes, deposited microarray data sets for cell lines in which X-inactivation status was already examined are used, and the X/A ratios are plotted as controls. The remaining lanes show X/A ratios from the same lines used in Figure 1. The X/A ratios are also shown in Table S1.
(H) X/A ratios from undifferentiated (Undiff) and differentiated (Diff) hESCs and hiPSCs and primary human endothelial cells from biopsy. Colors signify independent cell lines, with the sex of the donor as indicated under the plot. For primary endothelial cells (Primary) only, red and purple are female, and green is male. The X/A ratios from the undifferentiated hESCs and hiPSCs were also used in Figure 1G.
(I) RNA FISH for *XIST* (red) and *PGK1* (green) in endothelial cells differentiated from indicated Xa/Xa hiPSC lines. Undifferentiated Xa/Xi hESC line ESI03 and Xa/Xa hiPSC line K-3F-2 serve as controls.
(J) Graph showing the proportion of cells exhibiting 0, 1, or 2 sites of PGK1 nascent mRNA accumulation in undifferentiated (K-3F-2; left) and differentiated (K-3F-2 and 3S-5F-4) hiPSCs. Five to fifteen percent of differentiated cells exhibit tetraploidy, similar to the proportion of these cells that exhibit two sites of PGK1 nascent mRNA accumulation.
The y axis in (G) and (H) is in $\log_2$ scale.

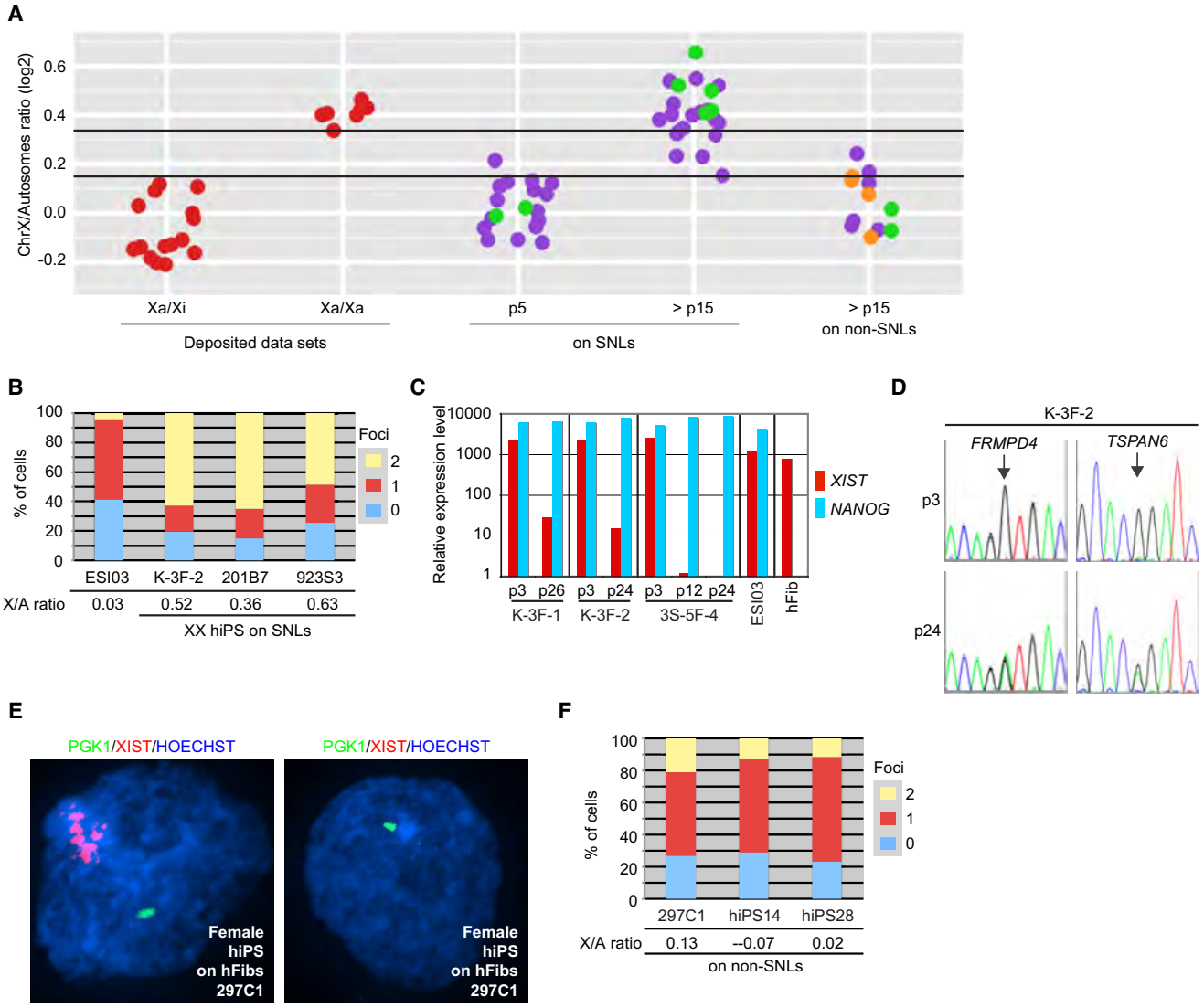

Figure 3. Prolonged Culture Promotes X-Reactivation When Propagated on SNL Feeders

(A) X/A ratios from hFib-derived female hiPSC lines at p5 or >p15. Cell lines were generated on SNLs or on non-SNLs. X/A ratios from hiPSC lines in which X-inactivation status was further examined in Figure 3 by FISH and/or SNP sequencing are shown in green, including three cell lines used in Figure 1 and Figure 2. Those examined in Figure 4 are shown in orange. X/A ratios from deposited Xa/Xi and Xa/Xa cell lines are shown in red. Cell lines above the upper black line in the graph have a predicted probability of at least 0.95 of being Xa/Xa, while those below the lower black line have a predicted probability of at least 0.95 of being Xa/Xi or a 0.05 probability of being Xa/Xa (see more details in Figure S2 and Supplemental Experimental Procedures). The X/A ratios are also shown in Table S1. The y axis is in $\log_2$ scale.

(B) Graph showing the proportion of cells exhibiting 0, 1, or 2 sites of PGK1 nascent mRNA accumulation in Xa/Xi hESCs (ESI03) and three hiPSC lines (K-3F-2, 201B7, and 923S3) on SNLs at >p15. X/A ratios from indicated lines are also shown.

(C) Relative expression levels of *XIST* and *NANOG*. RNA from the three hiPSC lines (K-3F-1, K-3F-2, and 3S-5F-4) was extracted at indicated passage number and analyzed by RT-qPCR. *NANOG* was used as a pluripotency marker. The Xa/Xi hESC line (ESI03) and female fibroblasts (hFib) from which the hiPSCs were generated served as controls. The y axis is in logarithmic scale. Expression values of *XIST* in 3S-5F-4 at p24 and of *NANOG* in hFib were set as 1.0.

(D) SNP sequencing of two X-linked genes (*TSPAN6* and *FRMPD4*) in one hiPSC line K-3F-2 on SNLs at p3 and p24. Arrows show position of SNPs.

(E) RNA FISH for *PGK1* (green) and *XIST* (red) in hiPSCs derived on hFibs. The hiPSC line 297C1 contains a mixed population of cells that do and do not express *XIST*.

(F) Graph showing the proportion of cells with 0, 1, or 2 sites of PGK1 nascent mRNA accumulation in three hiPSC lines generated and cultured on non-SNLs at >p12. X/A ratios are included beneath the graph.

humans (Okamoto et al., 2011; van den Berg et al., 2009). Our hiPSCs may overcome these challenges.

The role of *XIST* during X-inactivation is not clear in human cells. Our hiPSC lines exhibited X-inactivation upon differentiation. However, there was no detectable *XIST* expression in the resulting purified endothelial cells. While it is unusual for differentiated cells not to express *XIST*, this noncoding RNA is not necessary for maintenance of X-inactivation (Brown and Willard, 1994) and can

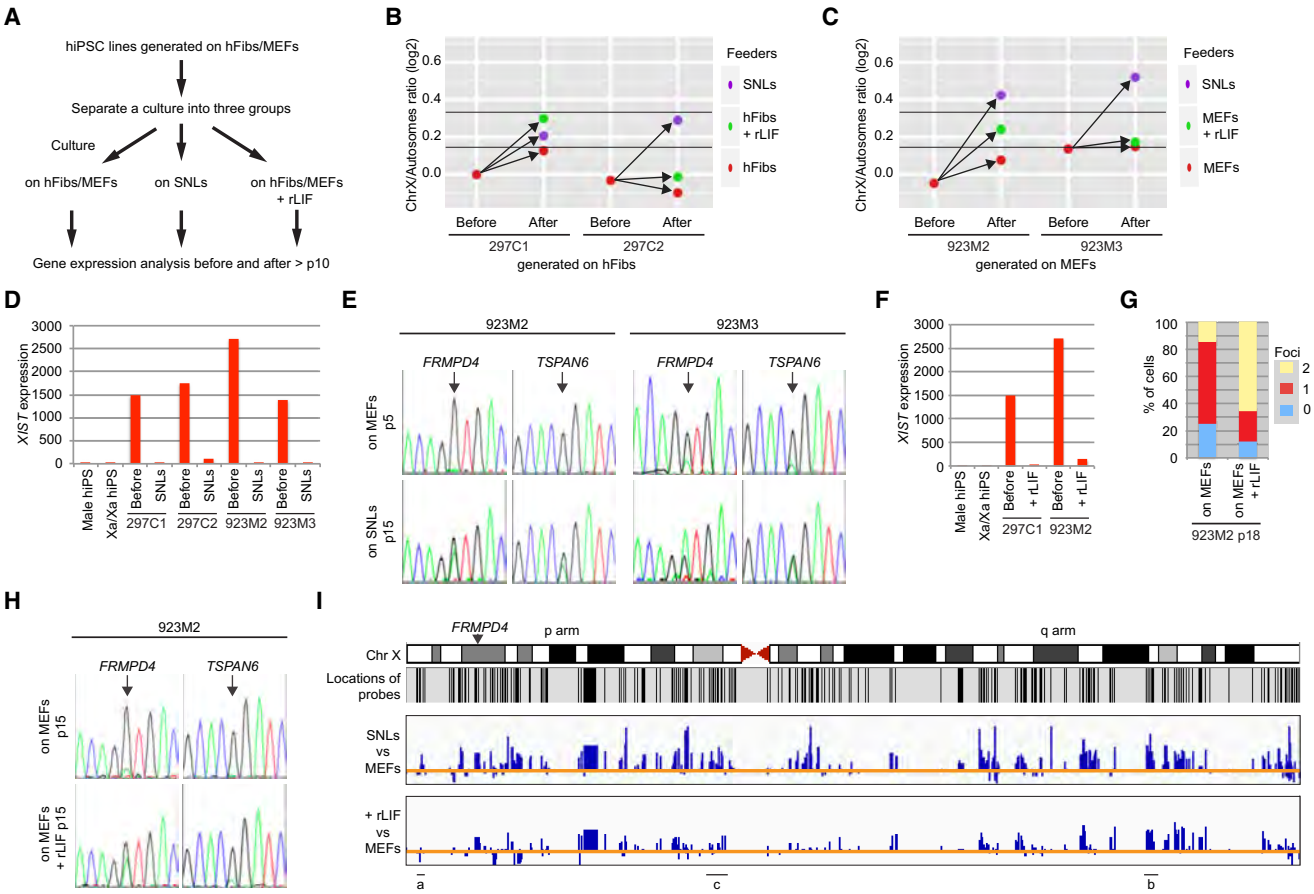

Figure 4. SNLs Have a Role in X-Reactivation in Female hiPSCs

(A) Diagram outlining experimental design. Related experiments are also shown in Figure S3.

(B and C) X/A ratios of hiPSC lines generated on non-SNLs and cultured as in Figure 4A. "Before" indicates ratios at p9 (B) and p3 (C), and "After" indicates ratios at >p15 under the conditions indicated in Figure 4A. According to our model, cell lines above the upper black line in the graph have a 0.95 probability of being Xa/Xa, and those below the lower black line have a 0.95 probability of being Xa/Xi. The y axis is in $\log_2$ scale.

(D and F) Normalized *XIST* expression in hiPSCs before and after transfer to SNLs (D) or before and after transfer to rLIF (F).

(E and H) SNP sequencing for *FRMPD4* and *TSPAN6* in hiPSCs before (p5) and after (p15) transfer to SNLs (E) or p15 hiPSCs on MEFs or MEFs plus rLIF (H). The hiPSC line 923M3 exhibits some biallelic expression of both genes at p5 on MEFs, consistent with both genes escaping X-inactivation at low frequency (Carrel and Willard, 2005).

(G) Graph showing the proportion of cells with 0, 1, or 2 sites of PGK1 nascent mRNA accumulation in indicated conditions.

(I) X-linked gene expression ratios plotted on the X. The probe locations are shown under the X diagram (note that many regions of the X do not have probes). The ratios of SNL hiPSCs and MEF hiPSCs (top bar chart) or between MEF plus rLIF hiPSCs and MEF hiPSCs (bottom bar chart) in hiPSC 923M2 are shown as bar charts. Each blue bar shows ratios for each gene analyzed. Blue bars above the orange line show upregulated genes in SNL hiPSCs or MEF plus rLIF hiPSCs compared with MEF hiPSCs, and below the orange line, they show downregulated genes. Line labeled (a) indicates a region of the X where gene expression on MEFs and MEFs plus rLIF is comparable, (b) indicates a region where genes are upregulated to a similar extent on SNLs and MEFs plus rLIF, and (c) indicates a region where genes are upregulated to a lesser degree on MEFs plus rLIF than on SNLs. Location of *FRMPD4* is indicated with an arrowhead.

be epigenetically silenced in cultured cells, including hESCs (Shen et al., 2008; Silva et al., 2008; Tchieu et al., 2010). Further analyses of our hiPSCs could provide new insights into regulation of *XIST* expression and X-inactivation in humans.

EXPERIMENTAL PROCEDURES

Extended Experimental Procedures are described in the Supplemental Information.

hiPSC Generation and Cell Culture

All hiPSC lines were generated by established protocols (http://www.cira.kyoto-u.ac.jp/e/research/protocol.html). All hESC lines were obtained from the National Stem Cell Bank (WiCell). hiPSC and hESC lines (Table S1) were maintained using standard protocols (Takahashi et al., 2007), with the exception that human insulin-like growth factor II (Chemicon; 33 ng/ml) was added into the ESC medium at Gladstone. Recombinant human LIF (Millipore; 10 ng/ml) was added into the medium as indicated. All karyotyping was performed at StemCell Technology, USA, or the Nihon Gene Research Laboratories, Japan. In all instances, passage 1 (p1) refers to when colonies are initially picked. SNL feeder cells are available at Health Protection Agency Culture Collection (http://www.hpacultures.org.uk/products/celllines/generalcell/detail.jsp?refId = 07032801&collection = ecacc_gc).

Microarray and Bioinformatics

Microarray (Whole Human Genome Microarray 4 × 44K or G3, Agilent) analyses were performed as described (Takahashi et al., 2007). All gene

expression values were normalized by the 75% percentile shift method. In Figures 1B and 1E, all probes of the microarrays were used for heat maps. In Figures S3A and S3B, only probes, which were used for calculating X/A ratios in Figures 4B and 4C, were used for heat maps. In Figures 1E, 4I, and S3C, IGV software (Broad Institute) was used. For Figure 1E, the expression ratios were calculated with averaged data from female hESC (ESI03, H7, H9, and H9-reporter) and hiPSC (K-3F-1, K-3F-2, and 3S-5F-4) lines. For Figures 4I and S3C, the expression ratios were calculated using selected data that were also used for Figures 4B and 4C. The microarray data for the deposited Xa/Xi and Xa/Xa lines used were downloaded from NCBI GEO (GEO numbers: GSE21222 and GSE22246).

ACCESSION NUMBERS

We have deposited the microarray data of hiPSC and hESC lines to GEO DataSets with the accession number GSE34527.

SUPPLEMENTAL INFORMATION

Supplemental Information for this article includes three figures, one table, and Supplemental Experimental Procedures and can be found with this article online at doi:10.1016/j.stem.2012.05.019.

ACKNOWLEDGMENTS

We thank members of the Yamanaka laboratory for useful discussions, Tim Rand for plotting the results of bisulfite sequencing and X/A ratios, Kenta Nakamura for hiPSC differentiation and useful discussions, Laura Mitic for maintaining the confocal microscope, Lei Lue for the endothelial cell differentiation, Michiyo Koyanagi for microarray analyses, Mari Ohnuki for discussion of neural differentiation, Gary Howard and Anna Lisa Lucido for editorial review, Karena Essex for administrative supports, Stem Cell Core for providing stem cell culture services, and Bioinformatics Core for conducting the statistic analyses. We also would like to thank Kathrin Plath and Sanjeet Patel for providing their hiPSC lines. K.T. is a scholar of the California Institute for Regenerative Medicine (CIRM). K.L. is supported by an NIH fellowship (F32 GM099389-01A1). B.P. is funded by NIH R01 GM088506. This work was supported in part by grants from the Leading Project of MEXT (Japan, to S.Y.), the Funding Program for World-Leading Innovative R&D on Science and Technology (FIRST Program) of the JSPS (Japan, to S.Y.), Grants-in-Aid for Scientific Research of the JSPS and MEXT (Japan, to S.Y.), and the Program for Promotion of Fundamental Studies in Health Sciences of NIBIO (Japan, to S.Y.). These studies were also made possible by funding from the Gladstone Institutes, the L.K. Whittier Foundation, NHLBI/NIH (U01-HL100406, U01-HL098179), and the CIRM. The Gladstone Institutes received support from a National Center for Research Resources Grant RR18928-01. S.Y. is a member without salary of the Scientific Advisory Board of iPierian, iPS Academia Japan, and Megakaryon Corporation; D.S. is a member of the Scientific Advisory Board of iPierian, Inc. and RegeneRx Pharmaceuticals; B.R.C. is a member of the Scientific Advisory Board of iPierian, Inc.; and N.A.Y. and P.T. are employees of Agilent Technologies, Inc.

Received: October 27, 2011
Revised: April 19, 2012
Accepted: May 15, 2012
Published: July 6, 2012

REFERENCES

Blanchard, F., Raher, S., Duplomb, L., Vusio, P., Pitard, V., Taupin, J.L., Moreau, J.F., Hoflack, B., Minvielle, S., Jacques, Y., and Godard, A. (1998). The mannose 6-phosphate/insulin-like growth factor II receptor is a nanomolar affinity receptor for glycosylated human leukemia inhibitory factor. J. Biol. Chem. *273*, 20886–20893.

Brown, C.J., and Willard, H.F. (1994). The human X-inactivation centre is not required for maintenance of X-chromosome inactivation. Nature *368*, 154–156.

Bruck, T., and Benvenisty, N. (2011). Meta-analysis of the heterogeneity of X chromosome inactivation in human pluripotent stem cells. Stem Cell Res. (Amst.) *6*, 187–193.

Carrel, L., and Willard, H.F. (2005). X-inactivation profile reveals extensive variability in X-linked gene expression in females. Nature *434*, 400–404.

Cheung, A.Y., Horvath, L.M., Grafodatskaya, D., Pasceri, P., Weksberg, R., Hotta, A., Carrel, L., and Ellis, J. (2011). Isolation of MECP2-null Rett Syndrome patient hiPS cells and isogenic controls through X-chromosome inactivation. Hum. Mol. Genet. *20*, 2103–2115.

Fan, G., and Tran, J. (2011). X chromosome inactivation in human and mouse pluripotent stem cells. Hum. Genet. *130*, 217–222.

Hanna, J., Cheng, A.W., Saha, K., Kim, J., Lengner, C.J., Soldner, F., Cassady, J.P., Muffat, J., Carey, B.W., and Jaenisch, R. (2010). Human embryonic stem cells with biological and epigenetic characteristics similar to those of mouse ESCs. Proc. Natl. Acad. Sci. USA *107*, 9222–9227.

Heard, E., and Disteche, C.M. (2006). Dosage compensation in mammals: fine-tuning the expression of the X chromosome. Genes Dev. *20*, 1848–1867.

Hoffman, L.M., Hall, L., Batten, J.L., Young, H., Pardasani, D., Baetge, E.E., Lawrence, J., and Carpenter, M.K. (2005). X-inactivation status varies in human embryonic stem cell lines. Stem Cells *23*, 1468–1478.

Kim, K.Y., Hysolli, E., and Park, I.H. (2011). Neuronal maturation defect in induced pluripotent stem cells from patients with Rett syndrome. Proc. Natl. Acad. Sci. USA *108*, 14169–14174.

Lagarkova, M.A., Shutova, M.V., Bogomazova, A.N., Vassina, E.M., Glazov, E.A., Zhang, P., Rizvanov, A.A., Chestkov, I.V., and Kiselev, S.L. (2010). Induction of pluripotency in human endothelial cells resets epigenetic profile on genome scale. Cell Cycle *9*, 937–946.

Lengner, C.J., Gimelbrant, A.A., Erwin, J.A., Cheng, A.W., Guenther, M.G., Welstead, G.G., Alagappan, R., Frampton, G.M., Xu, P., Muffat, J., et al. (2010). Derivation of pre-X inactivation human embryonic stem cells under physiological oxygen concentrations. Cell *141*, 872–883.

Lin, H., Gupta, V., Vermilyea, M.D., Falciani, F., Lee, J.T., O'Neill, L.P., and Turner, B.M. (2007). Dosage compensation in the mouse balances up-regulation and silencing of X-linked genes. PLoS Biol. *5*, e326.

Maherali, N., Sridharan, R., Xie, W., Utikal, J., Eminli, S., Arnold, K., Stadtfeld, M., Yachechko, R., Tchieu, J., Jaenisch, R., et al. (2007). Directly reprogrammed fibroblasts show global epigenetic remodeling and widespread tissue contribution. Cell Stem Cell *1*, 55–70.

Marchetto, M.C., Carromeu, C., Acab, A., Yu, D., Yeo, G.W., Mu, Y., Chen, G., Gage, F.H., and Muotri, A.R. (2010). A model for neural development and treatment of Rett syndrome using human induced pluripotent stem cells. Cell *143*, 527–539.

McMahon, A.P., and Bradley, A. (1990). The Wnt-1 (int-1) proto-oncogene is required for development of a large region of the mouse brain. Cell *62*, 1073–1085.

Mekhoubad, S., Bock, C., de Boer, A.S., Kiskinis, E., Meissner, A., and Eggan, K. (2012). Erosion of Dosage Compensation Impacts Human iPSC Disease Modeling. Cell Stem Cell *10*, 595–609.

Nakagawa, M., Koyanagi, M., Tanabe, K., Takahashi, K., Ichisaka, T., Aoi, T., Okita, K., Mochiduki, Y., Takizawa, N., and Yamanaka, S. (2008). Generation of induced pluripotent stem cells without Myc from mouse and human fibroblasts. Nat. Biotechnol. *26*, 101–106.

Nguyen, D.K., and Disteche, C.M. (2006). Dosage compensation of the active X chromosome in mammals. Nat. Genet. *38*, 47–53.

Nichols, J., and Smith, A. (2009). Naive and primed pluripotent states. Cell Stem Cell *4*, 487–492.

Okamoto, I., Patrat, C., Thépot, D., Peynot, N., Fauque, P., Daniel, N., Diabangouaya, P., Wolf, J.P., Renard, J.P., Duranthon, V., and Heard, E. (2011). Eutherian mammals use diverse strategies to initiate X-chromosome inactivation during development. Nature *472*, 370–374.

Okita, K., Matsumura, Y., Sato, Y., Okada, A., Morizane, A., Okamoto, S., Hong, H., Nakagawa, M., Tanabe, K., Tezuka, K.I., et al. (2011). A more efficient method to generate integration-free human iPS cells. Nat. Methods. *8*, 409–412.

Payer, B., Lee, J.T., and Namekawa, S.H. (2011). X-inactivation and X-reactivation: epigenetic hallmarks of mammalian reproduction and pluripotent stem cells. Hum. Genet. *130*, 265–280.

Polo, J.M., Liu, S., Figueroa, M.E., Kulalert, W., Eminli, S., Tan, K.Y., Apostolou, E., Stadtfeld, M., Li, Y., Shioda, T., et al. (2010). Cell type of origin influences the molecular and functional properties of mouse induced pluripotent stem cells. Nat. Biotechnol. *28*, 848–855.

Pomp, O., Dreesen, O., Leong, D.F., Meller-Pomp, O., Tan, T.T., Zhou, F., and Colman, A. (2011). Unexpected X chromosome skewing during culture and reprogramming of human somatic cells can be alleviated by exogenous telomerase. Cell Stem Cell *9*, 156–165.

Shen, Y., Matsuno, Y., Fouse, S.D., Rao, N., Root, S., Xu, R., Pellegrini, M., Riggs, A.D., and Fan, G. (2008). X-inactivation in female human embryonic stem cells is in a nonrandom pattern and prone to epigenetic alterations. Proc. Natl. Acad. Sci. USA *105*, 4709–4714.

Silva, S.S., Rowntree, R.K., Mekhoubad, S., and Lee, J.T. (2008). X-chromosome inactivation and epigenetic fluidity in human embryonic stem cells. Proc. Natl. Acad. Sci. USA *105*, 4820–4825.

Takahashi, K., Tanabe, K., Ohnuki, M., Narita, M., Ichisaka, T., Tomoda, K., and Yamanaka, S. (2007). Induction of pluripotent stem cells from adult human fibroblasts by defined factors. Cell *131*, 861–872.

Takahashi, K., Narita, M., Yokura, M., Ichisaka, T., and Yamanaka, S. (2009). Human induced pluripotent stem cells on autologous feeders. PLoS ONE *4*, e8067.

Tchieu, J., Kuoy, E., Chin, M.H., Trinh, H., Patterson, M., Sherman, S.P., Aimiuwu, O., Lindgren, A., Hakimian, S., Zack, J.A., et al. (2010). Female human iPSCs retain an inactive X chromosome. Cell Stem Cell *7*, 329–342.

Teichroeb, J.H., Betts, D.H., and Vaziri, H. (2011). Suppression of the imprinted gene NNAT and X-chromosome gene activation in isogenic human iPS cells. PLoS ONE *6*, e23436.

van den Berg, I.M., Laven, J.S., Stevens, M., Jonkers, I., Galjaard, R.J., Gribnau, J., and van Doorninck, J.H. (2009). X chromosome inactivation is initiated in human preimplantation embryos. Am. J. Hum. Genet. *84*, 771–779.

Ware, C.B., Wang, L., Mecham, B.H., Shen, L., Nelson, A.M., Bar, M., Lamba, D.A., Dauphin, D.S., Buckingham, B., Askari, B., et al. (2009). Histone deacetylase inhibition elicits an evolutionarily conserved self-renewal program in embryonic stem cells. Cell Stem Cell *4*, 359–369.